Journal of Radiotherapy in Practice

cambridge.org/jrp

Retrospective analysis of portal dosimetry pre-treatment quality assurance of intracranial SRS/SRT VMAT treatment plans

Ernest Osei[1,2,3,4], Sarah Graves[1,2] and Johnson Darko[1,2,4]

[1]Department of Medical Physics, Grand River Regional Cancer Centre, Kitchener, ON, Canada; [2]Department of Physics and Astronomy, University of Waterloo, Waterloo, ON, Canada; [3]Department of Systems Design Engineering, University of Waterloo, Waterloo, ON, Canada and [4]Department of Clinical Studies, Ontario Veterinary College, University of Guelph, Guelph, ON, Canada

Original Article

Cite this article: Osei E, Graves S, and Darko J. (2022) Retrospective analysis of portal dosimetry pre-treatment quality assurance of intracranial SRS/SRT VMAT treatment plans. *Journal of Radiotherapy in Practice* **21**: 540–552. doi: 10.1017/S146039692100042X

Received: 27 March 2021
Revised: 12 June 2021
Accepted: 21 June 2021
First published online: 27 September 2021

Key words:
EPID; Gamma evaluation; patient-specific QA; SRS and SRT; VMAT

Author for correspondence:
Dr Ernest Osei, Department of Medical Physics, Grand River Regional Cancer Centre, 835 King Street West, Kitchener, ON, Canada. Tel: 519 749 4300. E-mail: ernest.osei@grhosp.onca

Abstract

Background: The complexity associated with the treatment planning and delivery of stereotactic radiosurgery (SRS) or stereotactic radiotherapy (SRT) volumetric modulated arc therapy (VMAT) plans which employs continuous dynamic modulation of dose rate, field aperture and gantry speed necessitates diligent pre-treatment patient-specific quality assurance (QA). Numerous techniques for pre-treatment VMAT treatment plans QA are currently available with the aid of several different devices including the electronic portal imager (EPID). Although several studies have provided recommendations for gamma criteria for VMAT pre-treatment QA, there are no specifics for SRS/SRT VMAT QA. Thus, we conducted a study to evaluate intracranial SRS/SRT VMAT QA to determine clinical action levels for gamma criteria based on the institutional estimated means and standard deviations.

Materials and methods: We conducted a retrospective analysis of 118 EPID patient-specific pre-treatment QA dosimetric measurements of 47 brain SRS/SRT VMAT treatment plans using the integrated Varian solution (RapidArc^{TM} planning, EPID and Portal dosimetry system) for planning, delivery and EPID QA analysis. We evaluated the maximum gamma (γ_{max}), average gamma (γ_{ave}) and percentage gamma passing rate (%GP) for different distance-to-agreement/dose difference (DTA/DD) criteria and low-dose thresholds.

Results: The gamma index analysis shows that for patient-specific SRS/SRT VMAT QA with the portal dosimetry, the mean %GP is ≥98% for 2–3 mm/1–3% and Field+0%, +5% and +10% low-dose thresholds. When applying stricter spatial criteria of 1 mm, the mean %GP is >90% for DD of 2–3% and ≥88% for DD of 1%. The mean γ_{max} ranges: 1·32 ± 1·33–2·63 ± 2·35 for 3 mm/1–3%, 1·57 ± 1·36–2·87 ± 2·29 for 2 mm/1–3% and 2·36 ± 1·83–3·58 ± 2·23 for 1 mm/1–3%. Similarly the mean γ_{ave} ranges: 0·16 ± 0·06–0·19 ± 0·07 for 3 mm/1–3%, 0·21 ± 0·08–0·27 ± 0·10 for 2 mm/1–3% and 0·34 ± 0·14–0·49 ± 0·17 for 1 mm/1–3%. The mean γ_{max} and mean γ_{ave} increase with increased DTA and increased DD for all low-dose thresholds.

Conclusions: The establishment of gamma criteria local action levels for SRS/SRT VMAT pre-treatment QA based on institutional resources is imperative as a useful tool for standardising the evaluation of EPID-based patient-specific SRS/SRT VMAT QA. Our data suggest that for intracranial SRS/SRT VMAT QA measured with the EPID, a stricter gamma criterion of 1 mm/2% or 1 mm/3% with ≥90% %GP could be used while still maintaining an in-control QA process with no extra burden on resources and time constraints.

Introduction

Cancers of the brain and the central nervous system (CNS) comprise a group of rare and heterogeneous tumours with respect to genetics and biology and account for approximately 3% of all cancer cases worldwide.[1] It was estimated that approximately 3,000 Canadians would be diagnosed with brain and CNS cancers and 2,500 would die from the disease in 2020.[2,3] In the USA, it was estimated that about 86,970 primary brain tumours (26,170 malignant and 60,800 benign cases) would be diagnosed in 2019 and 16,830 patients would die from malignant brain cancer.[4] Furthermore, according to the National Brain Tumor Society,[4] about 700,000 people in the USA are living with brain tumour (30·9% are malignant and 69·1% are benign tumours) and the average survival rate for all malignant brain tumour patients is estimated at 35%. The standard treatment modalities for brain cancer include surgery, radiation therapy, chemotherapy or any combination depending on tumour type, grade, location, size and age of patient. Whole brain radiotherapy (WBRT) using either parallel opposed beams or intensity-modulated radiation therapy (IMRT) technique has been used for the treatment of brain cancers.[5–9] However, in recent years, single fraction stereotactic radiosurgery (SRS) or fractionated stereotactic radiotherapy (SRT) has emerged as other treatment modalities and has proven to be extremely effective when treating brain metastases

both as a single treatment modality and/or in conjunction with WBRT.[7,9,10] The gold standard for the delivery of brain SRS has been the use of the gamma-knife technology;[11–15] however, due to the high cost, several Cancer Centers in recent years have opted to use Linac-based volumetric modulated arc therapy (VMAT), which employs continuous dynamic modulation of dose rate, field aperture and gantry speed, or IMRT or stereotactic cones to deliver brain SRS/SRT treatments.[7–9,16–23] Several studies have demonstrated that using VMAT for treatment of brain metastases is associated with reduced toxicity compared to whole-brain radiation therapy.[17–20]

The complexity associated with the planning and delivery processes for SRS/SRT VMAT treatment plans necessitates diligent pre-treatment patient-specific quality assurance (QA) to ensure that the treatment planning calculated doses can be delivered by the linear accelerator within acceptable tolerances of 2–3 mm/2–3%.[22–30] Several techniques for pre-treatment QA of SRS/SRT VMAT treatment plans are currently available using devices such as the ArcCHECK™ (Sun Nuclear Corporation, Melbourne, FL, USA), MAPCheck™ (Sun Nuclear Corporation, Melbourne, FL, USA), Delta4™ (ScandiDos AB, Uppsala, Sweden) and MatriXX™ (IBA Dosimetry GmbH, Schwarzenbruck, Germany).[22,30–35] In recent years, the use of the electronic portal imaging device (EPID) for pre-treatment patient-specific treatment plan verification has gained increased interest due to its simplicity.[22,23,26–29,35–39] The Varian EPID has been shown to be capable of producing high-resolution measured dose digital images which can be compared with predicted portal dose images calculated by the Eclipse™ Treatment Planning System (TPS) based on the actual fluence distribution for every patient treatment plan fields.[22,23,28–30,36,40,41] Various methods including the dose difference (DD), distance-to-agreement (DTA) and the gamma (γ) index have been used to compare the measured and predicted dose images.[22–24,26–30,35–39,42–44] The DD is the difference in dose at a specified point in each of the predicted and measured dose distributions, and it is reflected as a percentage of the maximum dose, whereas the DTA represents the nearest distance between two points of equal dose on the predicted and measured dose images when superimposed.[22,23,30,42,43,45] According to Low et al.[42] and Low & Dempsey,[43] the DD method is very sensitive in areas of high-dose gradient and a small spatial misalignment will cause a large DD between the measured and the calculated dose distributions, whereas the DTA method is sensitive in areas of low-dose gradient and a small DD in low-dose area could result in large DTA values. Consequently, it is a common practice to compare the predicted and measured dose distributions using the gamma (γ) index technique which takes both the DD and DTA into consideration.[22–24,26–30,35–39,42–44] This evaluation method indicates a satisfactory agreement between a specific dose point in the predicted and measured dose images when the dimensionless quantity γ is ≤1, otherwise the dose point is considered to fail.[22,24,30,42,43] The overall agreement of a set of predicted and measured dose distributions is characterised by the percentage of dose points that fulfil passing criteria, known as the gamma passing rate (%GP). In addition to the gamma passing rate, the maximum gamma (γ_{max}) and average gamma (γ_{ave}) values for a dose image comparison may be obtained to provide further insight into the respective dose distributions. The goal of this study was to evaluate the gamma index-based analysis performed for SRS/SRT VMAT treatment fields for six DTA/DD gamma criteria combinations ranging from 1 to 3 mm and 1–3% to investigate the influence of different gamma criteria on the gamma passing rate, maximum gamma and the average gamma. We also investigated the impact of different low-dose thresholds of Field+0%, +5% and +10% regions of interest on the gamma parameters.

Materials and Methods

We conducted a retrospective evaluation of 118 EPID patient-specific pre-treatment VMAT QA dosimetric measurements of 47 brain SRS/SRT patients treated at our Center from November 2019 to January 2020 using the integrated Varian solution (RapidArc™ planning, EPID and Portal dosimetry system) for planning, delivery and EPID QA analysis. Patient treatment plans were delivered on Varian TrueBeam linear accelerators (Varian Medical Systems, Palo Alto, CA, USA) equipped with 120 multi-leaf collimators. The EPID dose images were collected via one of two integrated amorphous silicon EPIDs: Varian PortalVision AS1000 (40 × 30 cm^2 flat-panel, matrix of 1,024 × 768 pixels and 0·392 mm pixel resolution) or Varian AS1200 (43 × 43 cm^2 flat-panel, matrix of 1,190 × 1,190 pixels and 0·336 mm pixel resolution) with the capability of integrated dose acquisition modes. The mechanical calibration of the EPID exact arms is done by our in-house electronic technology staff, and the EPID dosimetry configuration and calibration are done by medical physicists.

Treatment planning for intracranial SRS/SRT

The treatment plans for all patients were accomplished in the Eclipse™ TPS (Varian Medical Systems, Palo Alto, CA, USA). The segmentation of the target and all the normal organs at risk (OARs) structures was based on institutional guidelines and included the delineation of the target (i.e. gross tumour volume (GTV)) and the OARs (i.e. brainstem, lens of the eyes, optic chiasm and healthy brain) aided by a T1-weighted MRI images. The RapidArc™ treatment plans were generated using 6MV, 6MV-FFF or 10MV-FFF photon beams and consisted of two to four arc fields and a prescription of either a single dose of 15–20 Gy or fractionated dose of 25–30 Gy in 3–5 fractions. The GTV target coverage is considered acceptable when at least 99% of the GTV volume is covered by 100% of the prescribed dose ($V_{100\ PD} > 99\%$) and a maximum dose of 160% of the prescribed dose.

Patient-specific portal dosimetry QA

The basis of portal dosimetry is that for each treatment field, a predicted fluence image is calculated in the Eclipse™ TPS. The TPS calculates the expected fluence from EPID for the verification plan in terms of absolute pixel values. The verification plan is subsequently delivered on the EPID using an integrated image acquisition mode via the ARIA™ system on a TrueBeam™ Linac similar to the actual clinical plan but delivered in the QA mode. The details of the portal dosimetry QA processes including the portal dose prediction, portal dose measurements, portal dose analysis and calibration of the EPID have been reported in a previous study.[36]

Portal dose prediction

The portal dose prediction image for each treatment beam was calculated by superposing the patients' treatment beams onto the portal imager's geometry at 100 cm source-to-image distance (SID) using the Portal Dose Image Prediction Algorithm in the Eclipse™ TPS version 13.6 (Varian Medical Systems, Palo Alto, CA, USA). Separate portal dose prediction image was calculated for each arc field using the actual planned parameters (gantry angles, collimator rotation, field size, dynamic MLC sequence, dose rate and number of monitor units) as in the original field used for the patient treatment.

https://doi.org/10.1017/S146039692100042X Published online by Cambridge University Press

Portal dose measurements

All verification plans were delivered on Varian TrueBeam™ Linacs using the integrated image acquisition mode with the calibrated EPID at the same SID of 100 cm as used during the absolute calibration of the imager with no additional build up on the imager. Data were acquired with the gantry rotating (arc motion), while the EPID itself was static relative to the gantry. Daily QA is performed on all linear accelerators to ensure consistency in output, symmetry and flatness. The EPID was calibrated according to the vendor's specifications, with dark field, flood field and absolute dose calibration.[41] The EPID response was scaled such that 1 Calibrated Unit (CU) corresponds to 100 monitor units (MU) delivered by a 10×10 cm^2 open field at 100 cm SID. The diagonal profile correction (used to scale the off-axis pixel response after flood field flattening) was performed as recommended by Varian. The beam intensity profile was measured at d_{max} in water for a 40×40 cm^2 open field. This profile correction and absolute dose calibration are applied on each integrated image acquisition.

Portal dose analysis

The dedicated ARIA™ Portal Dosimetry Review workspace within the Eclipse™ TPS was used to evaluate the agreement between the predicted and measured images. Dosimetric analysis of the PortalVision dose images was performed through the Varian Portal Dosimetry Version 13.6. The gamma index concept in the portal dosimetry system was used to quantify the agreement between the predicted and measured images. The assumption made is that if the images agree within set accepted tolerances, then the treatment plan is dosimetrically deliverable by the treatment machine. The absolute gamma analyses were performed to obtain the gamma passing rate (%GP), maximum gamma (γ_{max}) and average gamma (γ_{ave}) for each beam in each patient treatment plan. The improved gamma calculation method in the Portal Dosimetry Version 13.6 was employed for all calculations, which allows for interpolation between neighbouring pixels when searching. Each image was assessed using three different regions of interest (ROIs), namely the Field+0%, +5% and +10% low-dose thresholds. In addition, we investigated the impact of 3 mm/3%, 3 mm/2%, 3 mm/1%, 2 mm/3%, 2 mm/2%, 2 mm/1%, 1 mm/3%, 1 mm/2% and 1 mm/1% DTA/DD criteria on the gamma passing rate, maximum gamma and average gamma.

Results

We retrospectively analysed 118 EPID patient-specific pre-treatment QA dosimetric measurements consisting of 47 intracranial cancer patients VMAT treatment plans. We evaluated the gamma index-based analysis performed for each VMAT field for six different DTA/DD criteria combinations ranging from 1 to 3 mm and 1–3% to investigate the influence of different gamma criteria on the %GP, γ_{max} and γ_{ave}. We also investigated the influence of the Field+0%, +5% and +10% low-dose thresholds' regions of interest on the gamma parameters. We used the concept of the equivalent spherical diameter of an irregularly shaped object to estimate the size of all targets using the relationship below:

$$d_{eqi} = 3\sqrt{\frac{6 * v}{\pi}}$$

where d_{eqi} is the equivalent spherical diameter of the target and v is the target volume. In this study, we stratified the targets sizes into four groups of $x \leq 1$ cm, 1 cm $< x \leq 2$ cm, 2 cm $< x \leq 3$ cm and $x > 3$ cm based on the equivalent spherical diameter of the targets.

Percentage gamma passing rate (%GP)

The distribution of the %GP stratified into the four different target sizes of $x \leq 1$ cm, 1 cm $< x \leq 2$ cm, 2 cm $< x \leq 3$ cm and $x > 3$ cm is represented by boxplots in Figures 1–4, respectively, for different low-dose thresholds. The boxplots (Figures 1–4) show the overall spread of the %GP (minimum−maximum), the lower quartile (Q1, i.e. 25th percentile), upper quartile (Q3, i.e. 75th percentile), the interquartile range (Q3-Q1), the mean, median and any %GP outliers (i.e. %GP data points that are located outside the whiskers of the boxplots). The interquartile range describes the middle 50% of the %GP when ordered from the lowest to highest, and it is often seen as a better measure of spread than the range as it is not influenced by %GP outliers. Tables 1–4 show a summary of the statistical analysis of the %GP stratified into target sizes of $x \leq 1$ cm, 1 cm $< x \leq 2$ cm, 2 cm $< x \leq 3$ cm and $x > 3$ cm, respectively, for different DTA/DD acceptance criteria and low-dose thresholds. A similar statistical analysis for all the target sizes combined is shown in Table 5. The gamma index analysis shows that for patient-specific intracranial SRS/SRT VMAT QA using the portal dosimetry, the overall mean %GP ranges: >99% for 3 mm/1–3%, 97·8 ± 2·4%–99·2 ± 1·3% for 2 mm/1–3%, 90·6 ± 9·1%–94·5 ± 6·1% for 1 mm/2–3% and 87·5 ± 10·0%–89·3 ± 9·3% for 1 mm/1% (Table 5).

Maximum gamma (γ_{max})

Figures 5a, 6a, 7a and 8a show bar charts of the mean γ_{max} for target sizes ≤1 cm, 1 cm $< x \leq 2$ cm, 2 cm $< x \leq 3$ cm and >3 cm, respectively, for different low-dose thresholds and DTA/DD criteria. The indicated error bars in the bar charts represent one standard deviation. A summary of the statistical analysis of the γ_{max} for all the target sizes ($n = 118$) at different gamma analysis DTA/DD criteria and for different low-dose thresholds is shown in Table 6. The gamma index analysis shows that for patient-specific intracranial SRS/SRT VMAT QA using the portal dosimetry, the mean γ_{max} ranges: 2·33 ± 2·37–4·25 ± 3·56 for 3 mm/1–3%, 2·72 ± 2·34–4·47 ± 3·41 for 2 mm/1–3% and 4·24 ± 2·94–5·24 ± 3·21 for 1 mm/1–3% for target sizes ≤1 cm (Figure 5a). Also for target sizes 1 cm $< x \leq 2$ cm, the mean γ_{max} ranges: 1·02 ± 0·47–2·10 ± 1·68 for 3 mm/1–3%, 1·24 ± 0·43–2·43 ± 1·70 for 2 mm/1–3% and 1·88 ± 0·53–3·12 ± 1·63 for 1 mm/1–3% (Figure 6a). For target sizes 2 cm $< x \leq 3$ cm, the mean γ_{max} ranges: 1·17 ± 0·48–2·58 ± 1·41 for 3 mm/1–3%, 1·37 ± 0·56–2·76 ± 1·37 for 2 mm/1–3% and 1·81 ± 0·70–3·52 ± 1·44 for 1 mm/1–3% (Figure 7a). And for target sizes >3 cm, the mean γ_{max} ranges: 0·77 ± 0·32–1·63 ± 1·04 for 3 mm/1–3%, 0·96 ± 0·31–1·76 ± 0·95 for 2 mm/1–3% and 1·43 ± 0·37–2·33 ± 0·98 for 1 mm/1–3% (Figure 8a). The mean γ_{max} is observed to increase with increased DTA and with increased DD for all low-dose thresholds. For the combined target sizes ($n = 118$), the overall mean γ_{max} ranges: 1·32 ± 1·33–2·63 ± 2·35 for 3 mm/1–3%, 1·57 ± 1·36–2·87 ± 2·29 for 2 mm/1–3% and 2·36 ± 1·83–3·58 ± 2·23 for 1 mm/1–3% for the low-dose threshold (Table 6).

Average gamma (γ_{ave})

The mean average gamma (γ_{ave}) for target sizes ≤1 cm, 1 cm $< x \leq 2$ cm, 2 cm $< x \leq 3$ cm and >3 cm is represented by bar charts in Figures 5b, 6b, 7b and 8b, respectively, for different low-dose thresholds and DTA/DD criteria. The indicated error bars in the

https://doi.org/10.1017/S146039692100042X Published online by Cambridge University Press

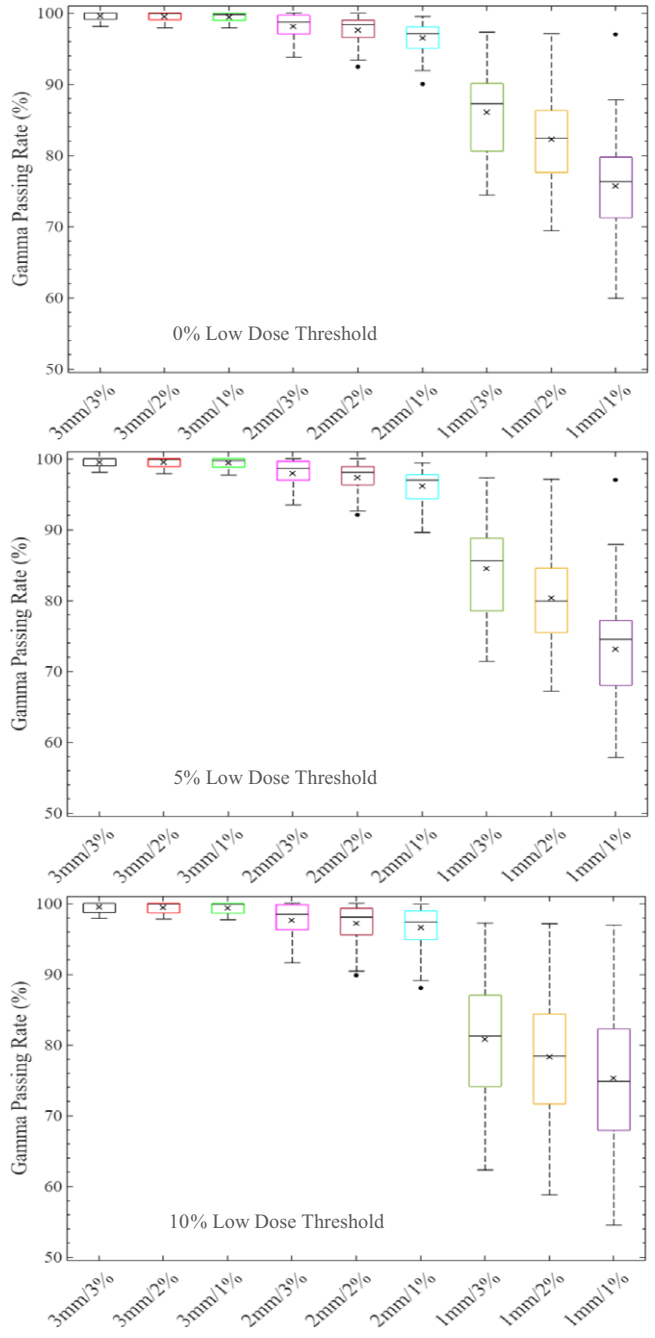

Figure 1. Boxplots of percentage gamma passing rates (%GP) for target sizes $x \leq 1$ cm at different gamma analysis distance-to-agreement and dose difference (DTA/DD) criteria and for Field+0%, +5% and +10% low-dose threshold regions of interest. The boxplots show the minimum, maximum, mean and median %GP, the lower quartile (Q1, i.e. 25th percentile), upper quartile (Q3, i.e. 75th percentile), interquartile range (Q3-Q1) and the %GP outliers (i.e. %GP data points that are located outside the whiskers of the boxplots). The interquartile range describes the middle 50% of the %GP when ordered from lowest to highest and is represented by the width of each box in the plot.

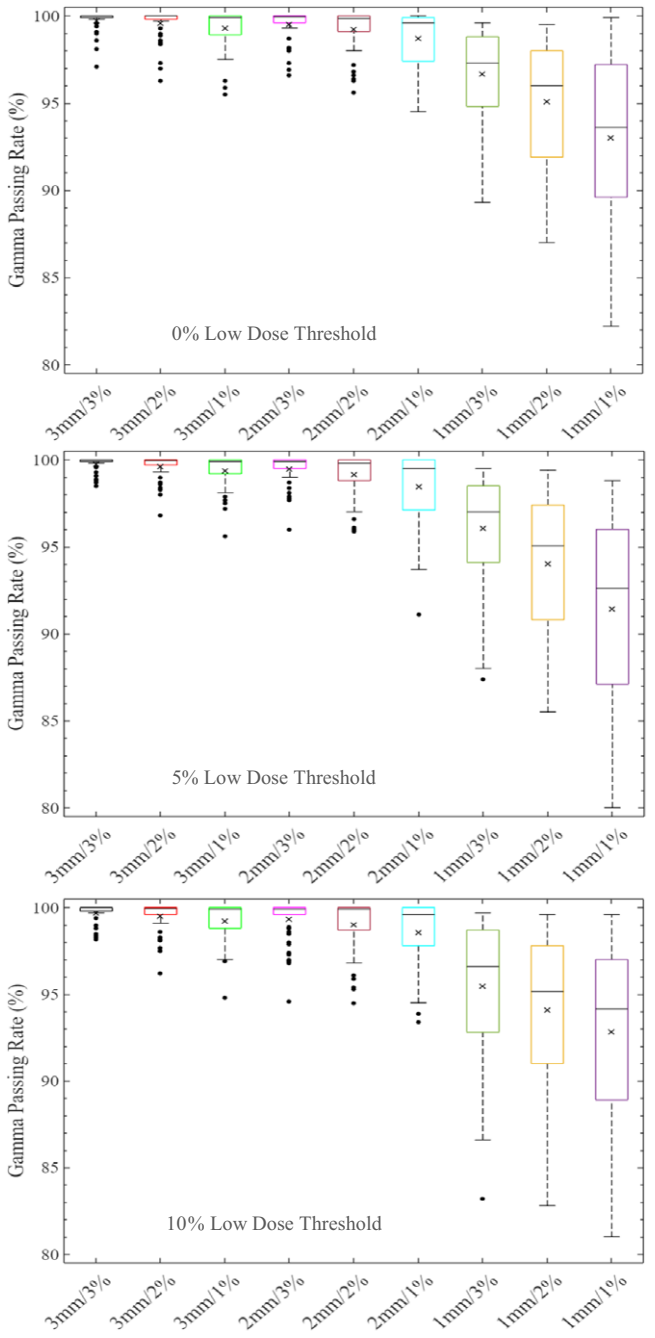

Figure 2. Boxplots of percentage gamma passing rates (%GP) for target sizes $1 \text{ cm} < x \leq 2$ cm at different gamma analysis distance-to-agreement and dose difference (DTA/DD) criteria and for Field+0%, +5% and +10% low-dose threshold regions of interest. The boxplots show the minimum, maximum, mean and median %GP, the lower quartile (Q1, i.e. 25th percentile), upper quartile (Q3, i.e. 75th percentile), interquartile range (Q3–Q1) and the %GP outliers (i.e. %GP data points that are located outside the whiskers of the boxplots). The interquartile range describes the middle 50% of the data when ordered from lowest to highest and is represented by the width of each box in the plot.

bar charts represent one standard deviation. A summary of the statistical analysis of the γ_{ave} for all target sizes ($n = 118$) at different gamma analysis DTA/DD criteria and for different low-dose threshold is shown in Table 6. The gamma index analysis shows that for patient-specific intracranial SRS/SRT VMAT QA using the portal dosimetry, the mean γ_{ave} ranges: 0·23 ± 0·04–0·27 ± 0·05 for 3 mm/1–3%, 0·32 ± 0·05–0·40 ± 0·07 for 2 mm/1–3% and 0·53 ± 0·10–0·70 ± 0·17 for 1 mm/1–3% for target sizes $x \leq 1$ cm (Figure 5b). Also for target sizes $1 \text{ cm} < x \leq 2$ cm, the mean γ_{ave} ranges: 0·14 ± 0·03–0·16 ± 0·05 for 3 mm/1–3%, 0·19 ± 0·05–0·24 ± 0·07 for 2 mm/1–3% and 0·30 ± 0·08–0·44 ± 0·10 for 1 mm/1–3% (Figure 6b). For target sizes $2 \text{ cm} < x \leq$

https://doi.org/10.1017/S146039692100042X Published online by Cambridge University Press

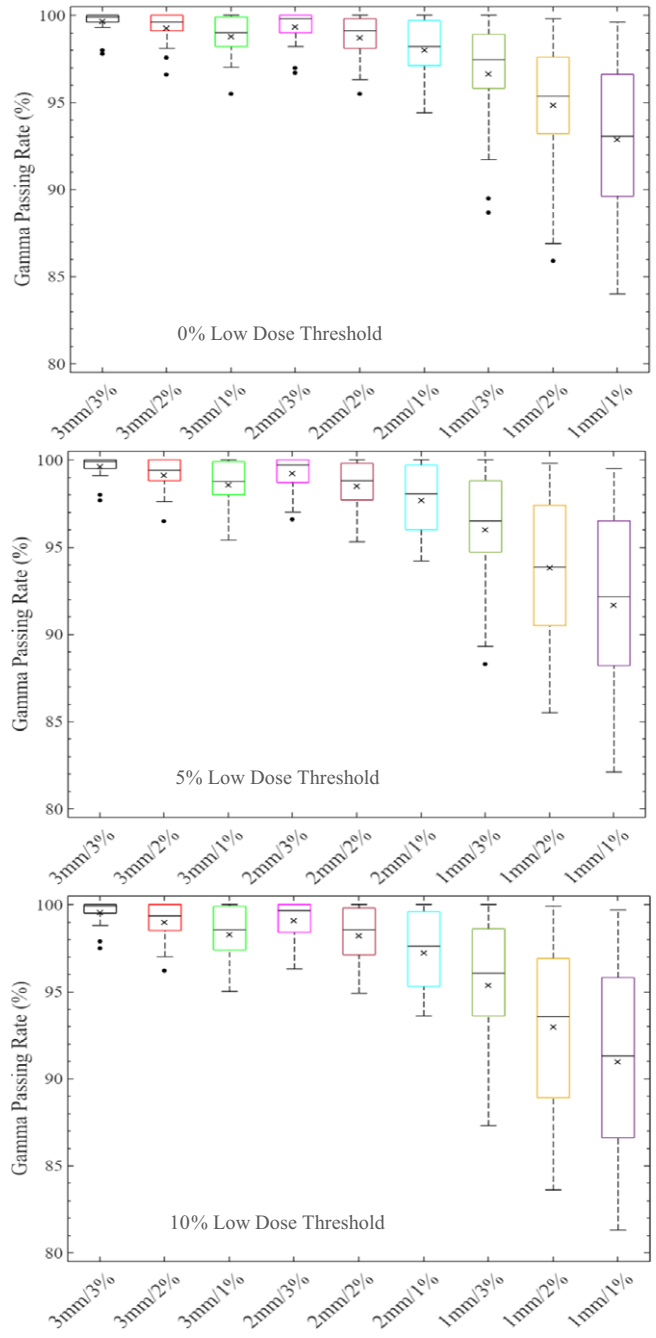

Figure 3. Boxplots of percentage gamma passing rates (%GP) for target sizes 2 cm < x ≤ 3 cm at different gamma analysis distance-to-agreement and dose difference (DTA/DD) criteria and for Field+0%, +5% and +10% low-dose threshold regions of interest. The boxplots show the minimum, maximum, mean and median %GP, the lower quartile (Q1, i.e. 25th percentile), upper quartile (Q3, i.e. 75th percentile), interquartile range (Q3–Q1) and the %GP outliers (i.e. %GP data points that are located outside the whiskers of the boxplots). The interquartile range describes the middle 50% of the data when ordered from lowest to highest and is represented by the width of each box in the plot.

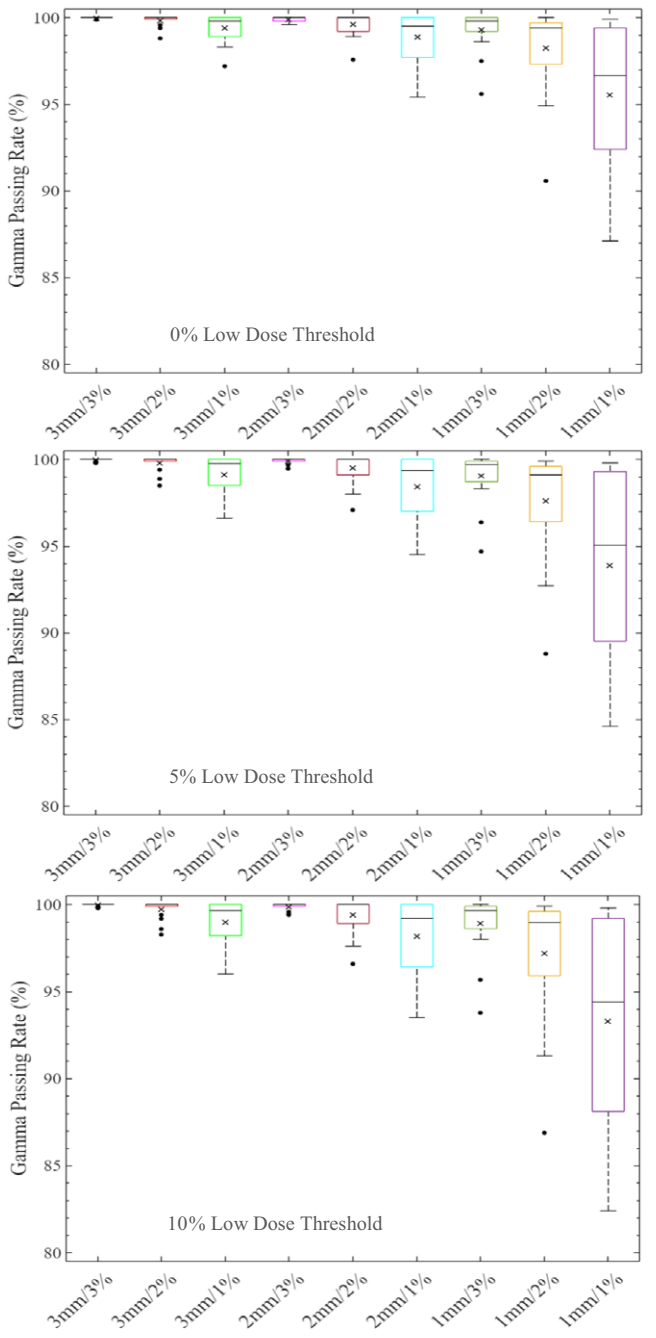

Figure 4. Boxplots of percentage gamma passing rates (%GP) for target sizes x > 3 cm at different gamma analysis distance-to-agreement and dose difference (DTA/DD) criteria and for Field+0%, +5% and +10% low-dose threshold regions of interest. The boxplots show the minimum, maximum, mean and median %GP, the lower quartile (Q1, i.e. 25th percentile), upper quartile (Q3, i.e. 75th percentile), interquartile range (Q3–Q1) and the %GP outliers (i.e. %GP data points that are located outside the whiskers of the boxplots). The interquartile range describes the middle 50% of the data when ordered from lowest to highest and is represented by the width of each box in the plot.

3 cm, the mean γ_{max} ranges: 0·14 ± 0·03–0·17 ± 0·06 for 3 mm/1–3%, 0·19 ± 0·05–0·24 ± 0·08 for 2 mm/1–3% and 0·30 ± 0·08–0·43 ± 0·13 for 1 mm/1–3% (Figure 7b). And for target sizes x > 3 cm, the mean γ_{max} ranges 0·10 ± 0·03–0·14 ± 0·06 for 3 mm/1–3%, 0·14 ± 0·04–0·20 ± 0·08 for 2 mm/1–3% and 0·21 ± 0·06–0·35 ± 0·12 for 1 mm/1–3% (Figure 8b). The mean γ_{ave} is observed to increase with increased DTA and also with increased DD for all low-dose thresholds. For the combined target sizes ($n = 118$), the overall mean γ_{ave} ranges: 0·16 ± 0·06–0·19 ± 0·07 for 3 mm/1–3%, 0·21 ± 0·08–0·27 ± 0·10 for 2 mm/1–3% and 0·34 ± 0·14–0·49 ± 0·17 for 1 mm/1–3% for all low-dose thresholds (Table 6).

https://doi.org/10.1017/S146039692100042X Published online by Cambridge University Press

Table 1. A summary of the statistical analysis of the percentage gamma passing rate for target sizes x ≤ 1 cm (n = 28) for different gamma analysis distance-to-agreement and dose difference (DTA/DD) criteria and for field+0%, +5% and +10% low-dose threshold regions of interest (ROIs)

	Percentage Gamma Passing Rate for various ROIs					
	0%		5%		10%	
Gamma Criteria (DTA/DD)	Mean ± SD	Range	Mean ± SD	Range	Mean ± SD	Range
3 mm/3%	99·6 ± 0·6	98·1–100·0	99·6 ± 0·6	98·1–100·0	99·5 ± 0·7	97·9–100·0
3 mm/2%	99·5 ± 0·6	97·9–100·0	99·5 ± 0·7	97·9–100·0	99·5 ± 0·7	97·8–100·0
3 mm/1%	99·5 ± 0·7	97·9–100·0	99·4 ± 0·7	97·7–100·0	99·4 ± 0·8	97·7–100·0
2 mm/3%	98·1 ± 1·7	93·8–100·0	98·0 ± 1·9	93·5–100·0	97·7 ± 2·4	91·6–100·0
2 mm/2%	97·6 ± 1·9	92·5–100·0	97·4 ± 2·1	92·1–100·0	97·2 ± 2·7	89·9–100·0
2 mm/1%	96·5 ± 2·3	90·1–99·5	96·2 ± 2·5	89·6–99·4	96·6 ± 3·1	88·1–99·9
1 mm/3%	86·1 ± 6·3	74·4–97·3	84·6 ± 6·7	71·4–97·3	80·9 ± 8·8	62·3–97·2
1 mm/2%	82·3 ± 6·8	69·4–97·1	80·4 ± 7·2	67·2–97·1	78·4 ± 9·4	58·8–97·1
1 mm/1%	75·7 ± 7·6	59·9–97·0	73·2 ± 8·3	57·8–97·0	75·3 ± 10·5	54·5–96·9

Table 2. A summary of the statistical analysis of the percentage gamma passing rate for target sizes 1 cm < x ≤ 2 cm ($n = 50$) for different gamma analysis distance-to-agreement and dose difference (DTA/DD) criteria and for field+0%, +5% and +10% low-dose threshold regions of interest (ROIs)

	Percentage Gamma Passing Rate for various ROIs					
	0%		5%		10%	
Gamma Criteria (DTA/DD)	Mean ± SD	Range	Mean ± SD	Range	Mean ± SD	Range
3 mm/3%	99·7 ± 0·6	97·1–100·0	99·8 ± 0·4	98·5–100·0	99·7 ± 0·6	98·2–100·0
3 mm/2%	99·6 ± 0·8	96·3–100·0	99·6 ± 0·7	96·8–100·0	99·5 ± 0·9	96·2–100·0
3 mm/1%	99·3 ± 1·2	95·5–100·0	99·4 ± 1·0	95·6–100·0	99·2 ± 1·2	94·8–100·0
2 mm/3%	99·5 ± 0·9	96·6–100·0	99·5 ± 0·9	96·0–100·0	99·4 ± 1·2	94·6–100·0
2 mm/2%	99·2 ± 1·2	95·6–100·0	99·2 ± 1·2	95·9–100·0	99·0 ± 1·5	94·5–100·0
2 mm/1%	98·7 ± 1·7	94·5–100·0	98·4 ± 2·1	91·1–100·0	98·6 ± 1·9	93·4–100·0
1 mm/3%	96·7 ± 2·6	89·3–99·6	96·1 ± 3·0	87·4–99·5	95·5 ± 3·8	83·2–99·7
1 mm/2%	95·1 ± 3·3	87·0–99·5	94·0 ± 3·8	85·5–99·4	94·1 ± 4·3	82·8–99·6
1 mm/1%	93·0 ± 4·6	82·2–99·9	91·4 ± 5·1	80·0–98·8	92·8 ± 5·1	81·0–99·6

Table 3. A summary of the statistical analysis of the percentage gamma passing rate for target sizes 2 cm < x ≤ 3 cm ($n = 22$) at different gamma analysis distance-to-agreement and dose difference (DTA/DD) criteria and for field+0%, +5% and +10% low-dose threshold regions of interest (ROIs)

	Percentage Gamma Passing Rate for various ROIs					
	0%		5%		10%	
Gamma Criteria (DTA/DD	Mean ± SD	Range	Mean ± SD	Range	Mean ± SD	Range
3 mm/3%	99·7 ± 0·6	97·8–100·0	99·6 ± 0·6	97·7–100·0	99·6 ± 0·7	97·5–100·0
3 mm/2%	99·3 ± 0·9	96·6–100·0	99·1 ± 1·0	96·5–100·0	99·0 ± 1·1	96·2–100·0
3 mm/1%	98·8 ± 1·2	95·5–100·0	98·6 ± 1·3	95·4–100·0	98·3 ± 1·5	95·0–100·0
2 mm/3%	99·3 ± 0·9	96·7–100·0	99·2 ± 1·0	96·6–100·0	99·1 ± 1·1	96·3–100·0
2 mm/2%	98·7 ± 1·3	95·5–100·0	98·5 ± 1·5	95·3–100·0	98·2 ± 1·7	94·9–100·0
2 mm/1%	98·0 ± 1·6	94·4–100·0	97·7 ± 1·9	94·2–100·0	97·2 ± 2·2	93·6–100·0
1 mm/3%	96·6 ± 3·2	88·7–100·0	96·0 ± 3·4	88·3–100·0	95·4 ± 3·9	87·3–100·0
1 mm/2%	94·8 ± 4·0	85·9–99·8	93·8 ± 4·3	85·5–99·8	93·0 ± 5·1	83·6–99·9
1 mm/1%	92·9 ± 4·5	84·0–99·6	91·7 ± 5·1	82·1–99·5	91·0 ± 5·8	81·3–99·7

https://doi.org/10.1017/S146039692100042X Published online by Cambridge University Press

Table 4. A summary of the statistical analysis of the percentage gamma passing rate for target sizes x > 3 cm ($n = 18$) at different gamma analysis distance-to-agreement and dose difference (DTA/DD) criteria and for field+0%, +5% and +10% low-dose threshold regions of interest (ROIs)

	Percentage Gamma Passing Rate for various ROIs					
	0%		5%		10%	
Gamma Criteria (DTA/DD)	Mean ± SD	Range	Mean ± SD	Range	Mean ± SD	Range
3 mm/3%	100·0 ± 0·0	99·9–100·0	100·0 ± 0·1	99·8–100·0	100·0 ± 0·1	99·8–100·0
3 mm/2%	99·9 ± 0·3	98·8–100·0	99·8 ± 0·4	98·5–100·0	99·7 ± 0·5	98·3–100·0
3 mm/1%	99·4 ± 0·8	97·2–100·0	99·1 ± 1·1	96·6–100·0	99·0 ± 1·3	96·0–100·0
2 mm/3%	99·9 ± 0·1	99·6–100·0	99·9 ± 0·2	99·5–100·0	99·9 ± 0·2	99·4–100·0
2 mm/2%	99·6 ± 0·6	97·6–100·0	99·5 ± 0·9	97·1–100·0	99·4 ± 1·0	96·6–100·0
2 mm/1%	98·9 ± 1·4	95·4–100·0	98·4 ± 1·9	94·5–100·0	98·2 ± 2·2	93·5–100·0
1 mm/3%	99·3 ± 1·1	95·6–100·0	99·0 ± 1·4	94·7–100·0	98·9 ± 1·7	93·8–100·0
1 mm/2%	98·2 ± 2·4	90·6–100·0	97·6 ± 3·0	88·8–99·9	97·2 ± 3·6	86·9–99·9
1 mm/1%	95·6 ± 4·0	87·1–99·9	93·9 ± 5·3	84·6–99·8	93·3 ± 6·0	82·4–99·8

Table 5. A summary of the statistical analysis of the percentage gamma passing rate for all target sizes ($n = 118$) at different gamma analysis distance-to-agreement and dose difference (DTA/DD) criteria and for field+0%, +5% and +10% low-dose threshold regions of interest (ROIs)

	Percentage Gamma Passing Rate for various low-dose threshold ROIs					
	0%		5%		10%	
Gamma Criteria (DTA/DD)	Mean ± SD	Range	Mean ± SD	Range	Mean ± SD	Range
3 mm/3%	99·7 ± 0·5	97·1–100·0	99·7 ± 0·5	97·7–100·0	99·7 ± 0·6	97·5–100·0
3 mm/2%	99·6 ± 0·8	96·3–100·0	99·5 ± 0·7	96·5–100·0	99·4 ± 0·9	96·2–100·0
3 mm/1%	99·3 ± 1·0	95·5–100·0	99·2 ± 1·1	95·4–100·0	99·1 ± 1·2	94·8–100·0
2 mm/3%	99·2 ± 1·3	93·8–100·0	99·1 ± 1·3	93·5–100·0	99·0 ± 1·7	91·6–100·0
2 mm/2%	98·8 ± 1·5	92·5–100·0	98·7 ± 1·7	92·1–100·0	98·5 ± 2·0	89·9–100·0
2 mm/1%	98·1 ± 2·0	90·1–100·0	97·8 ± 2·3	89·6–100·0	97·8 ± 2·4	88·1–100·0
1 mm/3%	94·5 ± 6·1	74·4–100·0	93·8 ± 6·7	71·4–100·0	92·5 ± 8·4	62·3–100·0
1 mm/2%	92·5 ± 7·3	69·4–100·0	91·3 ± 7·8	67·2–99·9	90·6 ± 9·1	58·8–99·9
1 mm/1%	89·3 ± 9·3	59·9–99·9	87·5 ± 10·0	57·8–99·8	88·4 ± 10·1	54·5–99·8

Discussion

In clinical practice, a common spatial/dose criterion of 3 mm/3% and a %GP of 90–95% have typically been used for both IMRT and VMAT pre-treatment QA.[46,47,49] The American Association of Physicists in Medicine (AAPM) Task Group 119 (TG 119) proposed using a spatial/dose criterion of 3 mm/3% with a low-dose threshold of 10% and a %GP of 90% for per beam analysis and 88–90% for composite irradiations.[46] Although, according to Stasi et al.,[49] when institutions use the 3%/3 mm criterion, the gamma passing rate action level most used is 95%. Several studies have questioned whether or not the 3 mm/3% criterion for patient-specific VMAT and IMRT pre-treatment QA is adequately sensitive, especially for small treatment fields <5 cm^2 or stricter criteria of 1–2 mm/1–3% should be considered in the clinical settings.[22,29,36,44,48,50–54] Steers and Frass[53] investigated an approach to quantitatively determine gamma criteria sensitivity to induced errors. They observed that errors as large as 15% MU errors and ± 1 cm random MLC errors can potentially be missed in IMRT QA with the commonly used gamma criteria of 3 mm/3%, 10% low-dose threshold and 90% gamma passing rate. Stasi et al.[49] also reported that the low sensitivity of 3 mm/3% global gamma method indicates that it has a disputable predictive power for per-patient IMRT QA. We previously reported that a stricter pre-treatment QA action level is required for VMAT QA for improved sensitivity.[29,36] According to Lechner et al.,[54] a stricter 3 mm/1% acceptance criterion than the standard 3%/3 mm must be used in small field dosimetry to accurately evaluate treatment delivery plans. Heilemann et al.[51] investigated the effects of small systematic MLC misalignments on the quality of VMAT QA verification measurements for prostate and head and neck treatment plans using the 2D-Array Seven29 (PTW-Freiburg, Germany) and the Delta4 (Scandidos). They demonstrated that the 3 mm/3% gamma index criterion is not sufficient to analyse VMAT plans and suggested using a stricter criterion of 2 mm/2% with passing rates >90% for both IMRT and VMAT plans pre-treatment QA. In a recent publication, the AAPM Task Group 218 (TG-218) published guidelines for pre-treatment QA and recommended a gamma criterion of 2 mm/3% with 10% low-dose threshold and %GP ≥ 90% for IMRT and VMAT QA.[48] Xia et al.[22] have

https://doi.org/10.1017/S146039692100042X Published online by Cambridge University Press

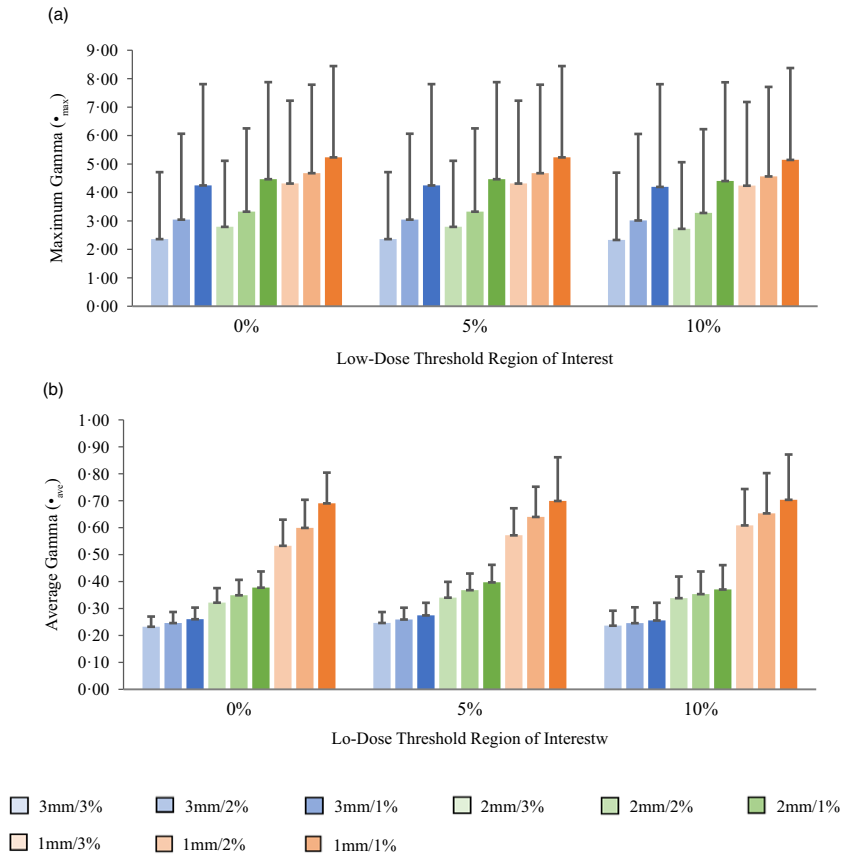

Figure 5. Bar charts of the maximum gamma (a) and average gamma (b) for target sizes x ≤ 1 cm at different gamma analysis distance-to-agreement and dose difference (DTA/DD) criteria for Field+0%, +5% and +10% low-dose threshold regions of interest.

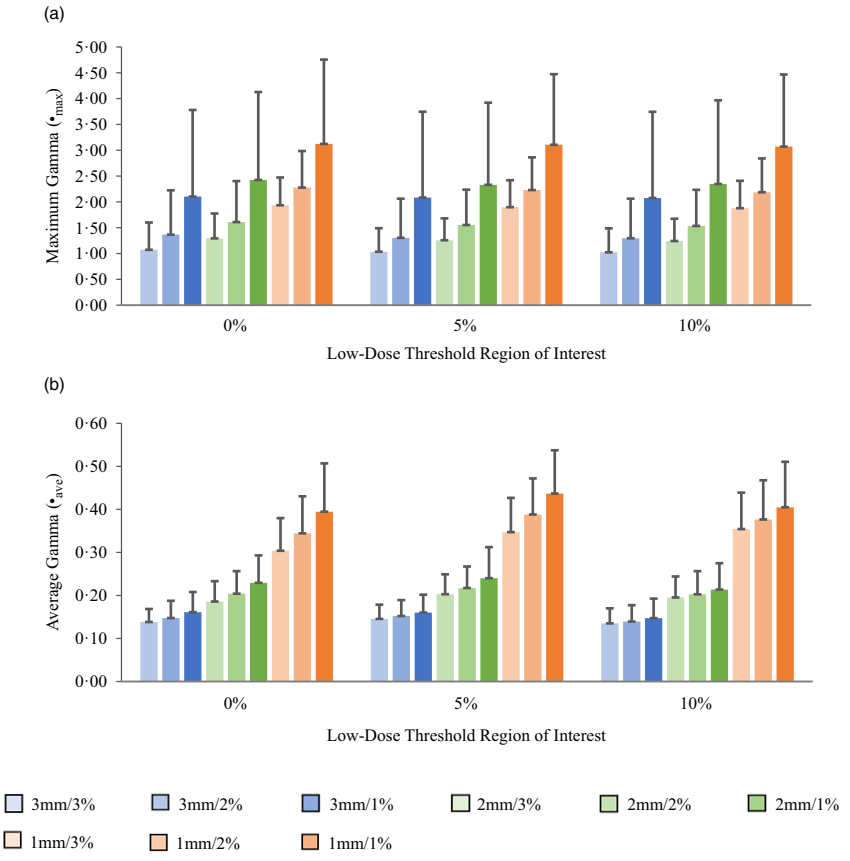

Figure 6. Bar charts of the maximum gamma (a) and average gamma (b) for target sizes 1 cm < x ≤ 2 cm at different gamma analysis distance-to-agreement and dose difference (DTA/DD) criteria for Field+0%, +5% and +10% low-dose threshold regions of interest.

https://doi.org/10.1017/S146039692100042X Published online by Cambridge University Press

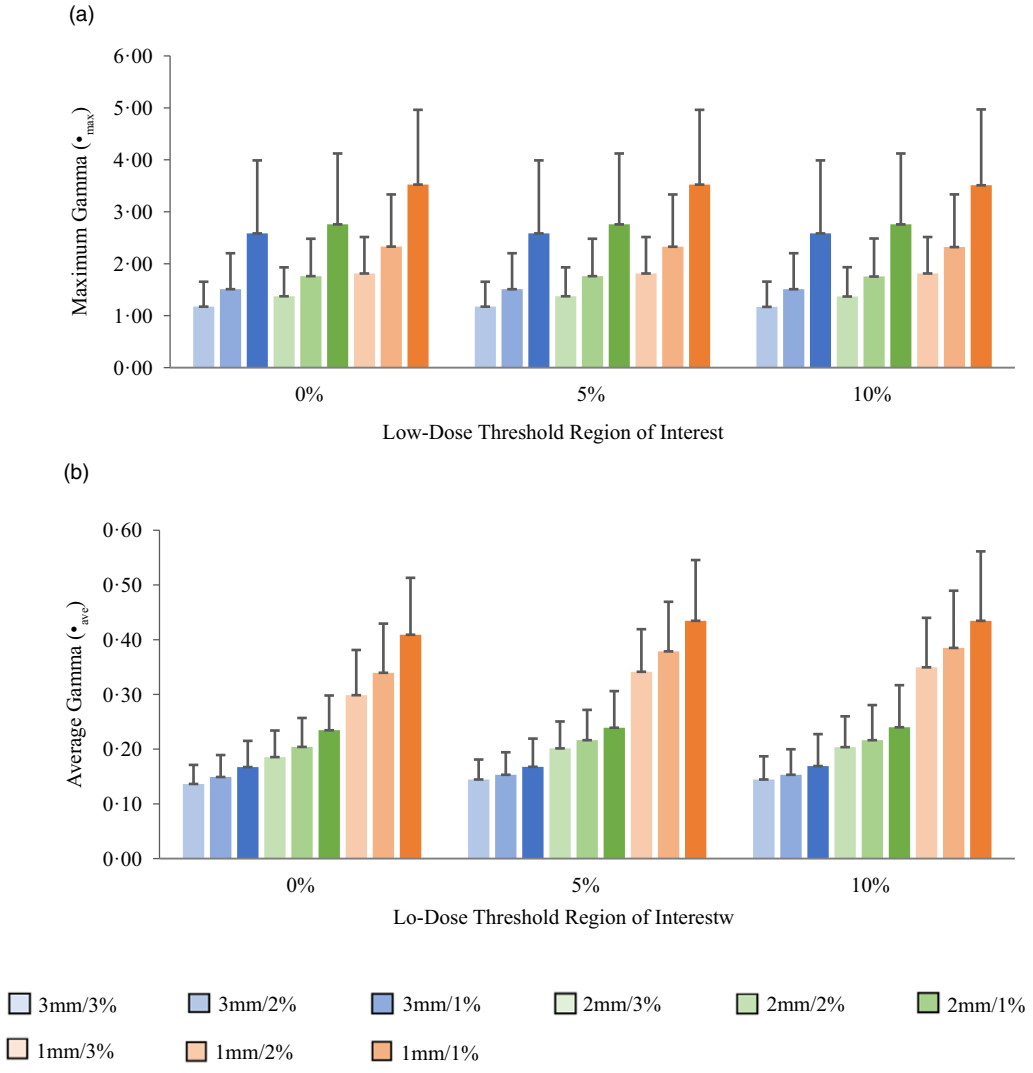

Figure 7. Bar charts of the maximum gamma (a) and average gamma (b) for target sizes 2 cm < x ≤ 3 cm at different gamma analysis distance-to-agreement and dose difference (DTA/DD) criteria for Field+0%, +5% and +10% low-dose threshold regions of interest.

also suggested a stricter criterion of 1 mm/3% with 10% low-dose threshold and %GP ≥ 90%. Our data suggest that the spatial tolerance criteria for brain SRS/SRT VMAT pre-treatment QA could be tightened to 1 mm while still maintaining an in-control QA process. Thus, it is possible to achieve a % GP ≥ 90% for SRS/SRT VMAT pre-treatment QA with 1 mm/2% or 1 mm/3% criterion with no extra burden on resources and time constraints. Kim et al.[50] investigated the sensitivity of several gamma criteria for patient-specific VMAT QA for SBRT treatment plans using the MapCHECK2 detector array (Sun Nuclear Corporation, Melbourne, FL, USA) and EBT2 film (Ashland Inc., Covington, KY, USA). They suggested that a gamma criterion of 1 mm/2% with passing rates of 90 and 80% should be used for patient-specific VMAT QA for SBRT when using MapCHECK2^{TM} and EBT2^{TM} film, respectively.

A number of studies have suggested using a combination of the average gamma, maximum gamma and the percentage gamma passing rate to analyse dose distributions and to make judgements regarding the agreement between measurements and calculation based on clinically driven criteria.[22,23,47,48,51,55–57] According to Miften et al.,[48] the analysis of the maximum gamma and the average gamma should be considered together with the percentage gamma passing rate for pre-treatment plan QA. Our data suggest an overall mean $\gamma_{ave} \leq 0{\cdot}19$ for 3 mm/1–3%, $\leq 0{\cdot}27$ for 2 mm/1–3% and $\leq 0{\cdot}49$ for 1 mm/1–3%; and an overall mean $\gamma_{max} \leq 2{\cdot}63$ for 3 mm/1–3%, $\leq 2{\cdot}87$ for 2 mm/1–3% and $\leq 3{\cdot}58$ for 1 mm/1–3% for patient-specific intracranial SRS/SRT VMAT pre-treatment QA using the portal dosimetry. Stock et al.[47] used a gamma criterion of 3%/3 mm to evaluate nine IMRT plans to decide on the acceptability of IMRT plan verification QA. They reported a mean γ_{ave} of $0{\cdot}45 \pm 0{\cdot}10$ and considered a plan to be acceptable if the average gamma <0·5, maximum gamma <1·5 and gamma passing rate >95%. Howell et al.[23] evaluated the maximum gamma and average gamma for 1152 treatment fields from 152 treatment plans and reported a mean γ_{max} of $2{\cdot}4 \pm 0{\cdot}8$ and a mean γ_{ave} of $0{\cdot}33 \pm 0{\cdot}13$. van Zijtveld et al.[58] also performed gamma analysis using a gamma criterion of 3%/3 mm and reported a mean γ_{ave} value of $0{\cdot}43 \pm 0{\cdot}13$ for 75 patients pre-treatment plan QA. Similarly, Atiq

https://doi.org/10.1017/S146039692100042X Published online by Cambridge University Press

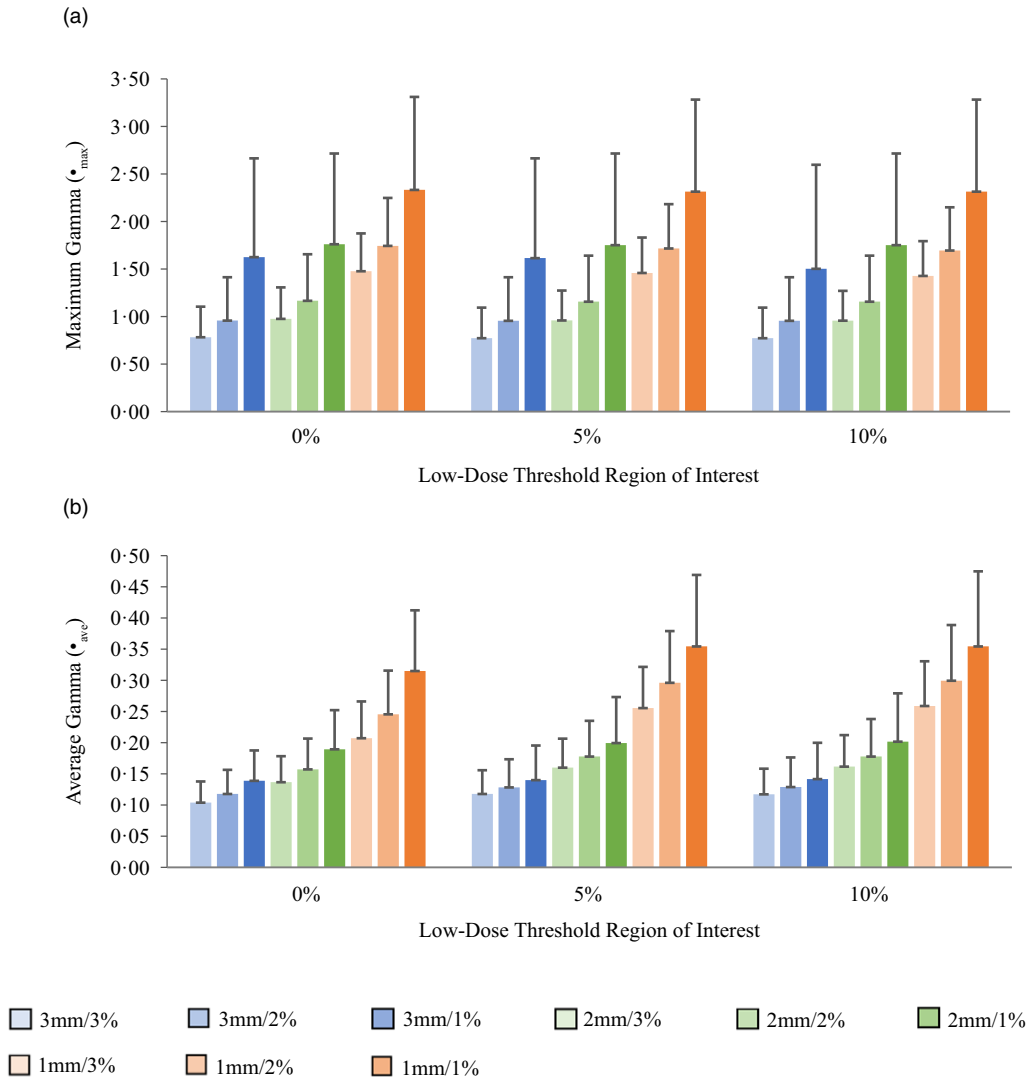

Figure 8. Bar charts of the maximum gamma (a) and average gamma (b) for target sizes x > 3 cm at different gamma analysis distance-to-agreement and dose difference (DTA/DD) criteria for Field+0%, +5% and +10% low-dose threshold regions of interest.

et al.[57] evaluated pre-treatment IMRT QA for 14 head and neck patients' treatment plans using the gamma analysis to investigate gamma criteria that assures a good quality plan and reported mean γ_{max} of 2·66 ± 2·38 and mean γ_{ave} of 0·30 ± 0·07 for 3 mm/5% gamma criterion.

Conclusion

Although there are several recommendations for gamma criteria for standard IMRT and VMAT pre-treatment QA, there are no specifics for intracranial SRS/SRT VMAT QA. The available criteria for standard VMAT may not be adequately sensitive for SRS/SRT VMAT techniques due to the high-dose gradients and small margins; thus, a tighter criterion may be necessary for SRS/SRT patient-specific VMAT QA. Our current data suggest that intracranial SRS/SRT VMAT QA can be accomplished using the EPID with stricter gamma criterion of 1 mm/2% or 1 mm/3% with % GP ≥ 90% with no extra burden on resources and time constraints.

The EPID is a convenient device for pre-treatment VMAT QA with its large high-resolution detector array, a linear response to radiation dose, and it is easily available as part of modern linear accelerators. It is capable of measuring high-resolution digital dose images without the need for a phantom or additional external devices. Furthermore, a typical pre-treatment VMAT QA procedure using EPID dosimetry only requires a single delivery of the patient QA plan, consequently making it an efficient tool in high patient-throughput radiotherapy clinics. Although the associated high Z component materials render EPIDs far from being water-equivalent compared to other ionisation chamber devices, it can effectively detect errors related to the delivery of dynamically modulated beams, e.g., MLC positioning errors, incorrect data transfer to the linear accelerator, and limitations or inaccuracies of the treatment planning system. Portal dosimetry is however limited in its ability to detect delivery errors associated with gantry position inaccuracies which can be dealt with in separate system level testing of the gantry position accuracy.

https://doi.org/10.1017/S146039692100042X Published online by Cambridge University Press

Table 6. A summary of the statistical analysis of maximum gamma and average gamma for all target sizes ($n = 118$) at different gamma analysis distance-to-agreement and dose difference (DTA/DD) criteria and for 0%, 5% and 10% low-dose threshold regions of interest (ROIs).

	Maximum Gamma and Average Gamma for various ROIs					
	0%		5%		10%	
Gamma Criteria (DTA/DD)	Mean ± SD	Range	Mean ± SD	Range	Mean ± SD	Range
	Maximum Gamma (γ_{max})					
3 mm/3%	1·35 ± 1·34	0·45–10·00	1·34 ± 1·33	0·45–10·00	1·32 ± 1·33	0·38–10·00
3 mm/2%	1·73 ± 1·76	0·46–10·00	1·70 ± 1·75	0·46–10·00	1·69 ± 1·75	0·46–10·00
3 mm/1%	2·63 ± 2·35	0·51–10·00	2·62 ± 2·35	0·51–10·00	2·59 ± 2·37	0·16–10·00
2 mm/3%	1·62 ± 1·37	0·61–10·00	1·60 ± 1·36	0·61–10·00	1·57 ± 1·36	0·53–10·00
2 mm/2%	1·98 ± 1·72	0·68–10·00	1·95 ± 1·71	0·68–10·00	1·93 ± 1·71	0·56–10·00
2 mm/1%	2·87 ± 2·29	0·73–10·00	2·83 ± 2·27	0·73–10·00	2·82 ± 2·29	0·69–10·00
1 mm/3%	2·41 ± 1·83	0·93–10·00	2·39 ± 1·84	0·93–10·00	2·36 ± 1·83	0·93–10·00
1 mm/2%	2·78 ± 1·96	1·07–10·00	2·75 ± 1·95	1·07–10·00	2·70 ± 1·95	1·06–10·00
1 mm/1%	3·58 ± 2·23	1·05–10·00	3·57 ± 2·16	1·36–10·00	3·53 ± 2·16	1·13–10·00
	Average Gamma (γ_{ave})					
3 mm/3%	0·16 ± 0·06	0·06–0·33	0·17 ± 0·06	0·07–0·34	0·16 ± 0·06	0·07–0·36
3 mm/2%	0·17 ± 0·06	0·06–0·35	0·17 ± 0·06	0·07–0·36	0·17 ± 0·06	0·07–0·38
3 mm/1%	0·18 ± 0·06	0·08–0·37	0·19 ± 0·07	0·07–0·39	0·18 ± 0·07	0·07–0·41
2 mm/3%	0·21 ± 0·08	0·06–0·45	0·23 ± 0·08	0·10–0·47	0·23 ± 0·09	0·09–0·51
2 mm/2%	0·23 ± 0·09	0·07–0·49	0·25 ± 0·09	0·10–0·51	0·24 ± 0·09	0·10–0·54
2 mm/1%	0·26 ± 0·09	0·10–0·53	0·27 ± 0·10	0·11–0·55	0·25 ± 0·10	0·10–0·58
1 mm/3%	0·34 ± 0·14	0·10–0·73	0·39 ± 0·14	0·16–0·78	0·40 ± 0·16	0·16–0·90
1 mm/2%	0·39 ± 0·15	0·11–0·83	0·43 ± 0·15	0·18–0·87	0·43 ± 0·17	0·18–0·98
1 mm/1%	0·46 ± 0·17	0·15–0·96	0·49 ± 0·17	0·10–0·99	0·47 ± 0·18	0·20–1·06

Acknowledgements. The authors would like to acknowledge with gratitude Nicholas Majtenyi for helping with the plotting of some of the Figures.

Conflicts of Interest. The authors declare that the research was conducted in the absence of any commercial or financial relationships that could be construed as a potential conflict of interest.

References

1. Miranda-Filho A, Pineros M, Soerjomataram I et al. Cancers of the brain and CNS: global patterns and trends in incidence. Neuro Oncol 2017; 19 (2): 270–280. doi: 10.1093/neuonc/now166
2. Brenner DR, Weir HK, Demers AA et al. Projected estimates of cancer in Canada in 2020. CMAJ 2020; 192 (9): E199–E205. doi: 10.1503/cmaj.191292
3. Canadian Cancer Society. Brain and spinal cord cancer statistics. https://www.cancer.ca/en/cancer-information/cancer-type/brain-spinal/statistics/?region=on. Accessed on February 06 2021, 2021.
4. National Brain Tumor Society. Brain tumors by the numbers. https://events.braintumor.org/wp-content/uploads/2019/02/BrainTumorsBytheNumbers_Jan_2019.pdf. Accessed on February 06 2021.
5. Park J, Park JW, Yea JW. Non-coplanar whole brain radiotherapy is an effective modality for parotid sparing. Yeungnam Univ J Med 2019; 36 (1): 36–42. doi: 10.12701/yujm.2019.00087. Epub 2019 Jan 3.
6. McTyre E, Scott J, Chinnaiyan P. Whole brain radiotherapy for brain metastasis. Surg Neurol Int 2013; 4 (Suppl 4): S236–S244. doi: 10.4103/2152-7806.111301
7. Sood S, Pokhrel D, McClinton C, Lominska C, Badkul R, Jiang H, Wang F. Volumetric-modulated arc therapy (VMAT) for whole brain radiotherapy: not only for hippocampal sparing, but also for reduction of dose to organs at risk. Med Dosim 2017; 42 (4): 375–383. doi: 10.1016/j.meddos.2017.07.005. Epub 2017 Aug 16.
8. Pokhrel D, Sood S, Kumar P et al. Volumetric modulated arc therapy (VMAT) significantly reduces treatment time and monitor units for whole-brain radiation therapy (WBRT) while still meeting RTOG Protocol 0933 hippocampal sparing constraints. Int J Radiat Oncol 2015; 93 (3): E621. doi: 10.1016/j.ijrobp.2015.07.2132
9. Remick JS, Kowalski E, Khairnar R et al. A multi-center analysis of single-fraction versus hypofractionated stereotactic radiosurgery for the treatment of brain metastasis. Radiat Oncol 2020; 15 (1): 128. doi: 10.1186/s13014-020-01522-6
10. Yamamoto M, Serizawa T, Shuto T et al. Stereotactic radiosurgery for patients with multiple brain metastases (JLGK0901): a multi-institutional prospective observational study. Lancet Oncol 2014; 15 (4): 387–395. doi: 10.1016/S1470-2045(14)70061-0. Epub 2014 Mar 10.
11. Jagannathan J, Petit JH, Balsara K, Hudes R, Chin LS. Long-term survival after gamma knife radiosurgery for primary and metastatic brain tumors. Am J Clin Oncol 2004; 27 (5): 441–444. doi: 10.1097/01.coc.0000128721.94095.e4
12. Matsunaga S, Shuto T, Kawahara N, Suenaga J, Inomori S, Fujino H. Gamma Knife surgery for brain metastases from colorectal cancer. Clinical article. J Neurosurg 2011; 114 (3): 782–789. doi: 10.3171/2010.9.JNS10354. Epub 2010 Oct 15.
13. Jagannathan J, Yen CP, Ray DK et al. Gamma Knife radiosurgery to the surgical cavity following resection of brain metastases. J Neurosurg 2009; 111 (3): 431–438. doi: 10.3171/2008.11.JNS08818
14. Serizawa T, Iuchi T, Ono J et al. Gamma knife treatment for multiple metastatic brain tumors compared with whole-brain radiation therapy. J Neurosurg 2000; 93 (Suppl 3): 32–36. doi: 10.3171/jns.2000.93.supplement

15. Gerosa M, Nicolato A, Foroni R et al. Gamma knife radiosurgery for brain metastases: a primary therapeutic option. J Neurosurg 2002; 97 (Suppl 5): 515–524. doi: 10.3171/jns.2002.97.supplement
16. Bas Ayata H, Ceylan C, Kılıç A, Güden M, Engin K. Comparison of multiple treatment planning techniques for high-grade glioma tumors near to critical organs. Oncol Res Treat 2018; 41: 514–519. doi: 10.1159/000487642
17. Zhang S, Yang R, Shi C et al. Noncoplanar VMAT for brain metastases: a plan quality and delivery efficiency comparison with coplanar VMAT, IMRT, and CyberKnife. Technol Cancer Res Treat 2019; 18: 1533033819871621. doi: 10.1177/1533033819871621
18. Yuen AHL, Wu PM, Li AKL, Mak PCY. Volumetric modulated arc therapy (VMAT) for hippocampal-avoidance whole brain radiation therapy: planning comparison with Dual-arc and Split-arc partial-field techniques. Radiat Oncol 2020; 15 (1): 42. doi: 10.1186/s13014-020-01488-5
19. Teoh M, Clark CH, Wood K, Whitaker S, Nisbet A. Volumetric modulated arc therapy: a review of current literature and clinical use in practice. Br J Radiol 2011; 84 (1007): 967–996. doi: 10.1259/bjr/22373346
20. Andrevska A, Knight KA, Sale CA. The feasibility and benefits of using volumetric arc therapy in patients with brain metastases: a systematic review. J Med Radiat Sci 2014; 61 (4): 267–276. doi: 10.1002/jmrs.69. Epub 2014 Sep 26.
21. Otto K. Volumetric modulated arc therapy: IMRT in a single gantry arc. Med Phys 2008; 35 (1): 310–317. doi: 10.1118/1.2818738
22. Xia Y, Adamson J, Zlateva Y, Giles W. Application of TG-218 action limits to SRS and SBRT pre-treatment patient specific QA. J Radiosurg SBRT 2020; 7 (2): 135–147.
23. Howell RM, Smith IPN, Jarrio CS. Establishing action levels for EPID-based QA for IMRT. J Appl Clin Med Phys 2008; 9 (3): 16–25. doi: 10.1120/jacmp.v9i3.2721
24. Low C, Toye W, Phung P, Huston C. Patient-specific quality assurance protocol for volumetric modulated arc therapy using dose volume histogram. J Med Phys 2018; 43 (2): 112–118. doi: 10.4103/jmp.JMP_138_17
25. Saito M, Kadoya N, Sato K et al. Comparison of DVH-based plan verification methods for VMAT: ArcCHECK-3DVH system and dynalog-based dose reconstruction. J Appl Clin Med Phys 2017; 18 (4): 206–214. doi: 10.1002/acm2.12123. Epub 2017 Jun 26.
26. Defoor DL, Quino LAV, Mavroidis P, Papanikolaou N, Stathakis S. Anatomy-based, patient-specific VMAT QA using EPID or MLC log files. J Appl Clin Med Phys 2015; 16 (3): 5283. doi: 10.1120/jacmp.v16i3.5283
27. Liang B, Liu B, Zhou F, Yin FF, Wu Q. Comparisons of volumetric modulated arc therapy (VMAT) quality assurance (QA) systems: sensitivity analysis to machine errors. Radiat Oncol 2016; 11 (1): 146. doi: 10.1186/s13014-016-0725-4
28. Liu B, Adamson J, Rodrigues A, Zhou F, Yin FF, Wu Q. A novel technique for VMAT QA with EPID in cine mode on a Varian TrueBeam linac. Phys Med Biol 2013; 58 (19): 6683–6700. doi: 10.1088/0031-9155/58/19/6683. Epub 2013 Sep 9.
29. Koo M, Darko J, Osei E. Retrospective analysis of portal dosimetry pretreatment quality assurance of hybrid IMRT breast treatment plans. J Radiother Pract. Cambridge University Press; 2021; 20 (1): 22–29.
30. Park JM, Kim J, Park SY et al. Reliability of the gamma index analysis as a verification method of volumetric modulated arc therapy plans. Radiat Oncol 2018; 13 (1): 175. doi: 10.1186/s13014-018-1123-x
31. Stojadinovic S, Ouyang L, Gu X, Pompoš A, Bao Q, Solberg TD. Breaking bad IMRT QA practice. J Appl Clin Med Phys 2015; 16 (3): 154–165. doi: 10.1120/jacmp.v16i3.5242
32. Nelms BE, Chan MF, Jarry G et al. Evaluating IMRT and VMAT dose accuracy: practical examples of failure to detect systematic errors when applying a commonly used metric and action levels. Med Phys 2013; 40 (11): 111722. doi: 10.1118/1.4826166
33. Hussein M, Rowshanfarzad P, Ebert MA, Nisbet A, Clark CH. A comparison of the gamma index analysis in various commercial IMRT/VMAT QA systems. Radiother Oncol 2013; 109 (3): 370–376. doi: 10.1016/j.radonc.2013.08.048. Epub 2013 Oct 4.
34. Vieillevigne L, Molinier J, Brun T, Ferrand R. Gamma index comparison of three VMAT QA Systems and evaluation of their sensitivity to delivery errors. Phys Med 2015; 31 (7): 720–725. doi: 10.1016/j.ejmp.2015.05.016. Epub 2015 Jun 19.
35. Bailey DW, Kumaraswamy L, Bakhtiari M, Malhotra HK, Podgorsak MB. EPID dosimetry for pretreatment quality assurance with two commercial systems. J Appl Clin Med Phys 2012; 13 (4): 3736. doi: 10.1120/jacmp.v13i4.3736
36. Maraghechi B, Davis J, Badu S, Fleck A, Darko J, Osei E. Retrospective analysis of portal dosimetry pre-treatment quality assurance of prostate volumetric-modulated arc therapy (VMAT) plans. J Radiother Pract. Cambridge University Press; 2018; 17 (1): 44–52.
37. Mohamed IE, Ibrahim AG, Zidan HM, El-Bahkiry HS, El-sahragti AY. Physical dosimetry of volumetric modulated arc therapy (VMAT) using EPID and 2D array for quality assurance. Egypt J Radiol Nucl Med 2018; 49(2): 477–484. doi: 10.1016/j.ejrnm.2018.02.003
38. Quino LAV, Chen X, Fitzpatrick M et al. Patient specific pre-treatment QA verification using an EPID approach. Technol Cancer Res Treat 2014; 13 (1): 1–10. doi: 10.7785/tcrt.2012.500351. Epub 2013 Jun 24.
39. Agarwal A, Rastogi N, Maria Das KJ, Yoganathan SA, Udayakumar D, Kumar S. Investigating the electronic portal imaging device for small radiation field measurements. J Med Phys 2017; 42 (2): 59–64. doi: 10.4103/jmp.JMP_131_16
40. Greer PB, Popescu CC. Dosimetric properties of an amorphous silicon electronic portal imaging device for verification of dynamic intensity modulated radiation therapy. Med Phys 2003; 30 (7): 1618–1627. doi: 10.1118/1.1582469
41. Varian Medical Systems. Portal Imaging and Portal Dosimetry Reference Guide. Palo Alto, CA, USA: Varian Medical Systems, 2008.
42. Low DA, Harms WB, Mutic S, Purdy JA. A technique for the quantitative evaluation of dose distributions. Med Phys 1998; 25 (5): 656–661. doi: 10.1118/1.598248
43. Low DA, Dempsey JF. Evaluation of the gamma dose distribution comparison method. Med Phys 2003; 30 (9): 2455–2464. doi: 10.1118/1.1598711.
44. Maraghechi B, Davis J, Mitchell N, Shah M, Fleck A, Darko J, Osei E. The sensitivity of gamma index analysis to detect multileaf collimator (MLC) positioning errors using Varian TrueBeam EPID and ArcCHECK for patient-specific prostate volumetric-modulated arc therapy (VMAT) quality assurance. J Radiother Pract. Cambridge University Press; 2018; 17 (1): 66–77.
45. Yeo IJ, Kim J. A procedural guide to film dosimetry: with emphasis on IMRT, 1st edition. Madison, WI: Medical Physics Publishing; 2004: 4.
46. Ezzell GA, Burmeister JW, Dogan N et al. IMRT commissioning: multiple institution planning and dosimetry comparisons, a report from AAPM Task Group 119. Med Phys 2009; 36: 5359–5373.
47. Stock M, Kroupa B, Georg D. Interpretation and evaluation of the gamma index and the gamma index angle for the verification of IMRT hybrid plans. Phys Med Biol 2005; 50 (3): 399–411. doi: 10.1088/0031-9155/50/3/001
48. Miften M, Olch A, Mihailidis D et al. Tolerance limits and methodologies for IMRT measurement-based verification QA: recommendations of AAPM Task Group No. 218. Med Phys 2018; 45 (4): e53–e83. doi: 10.1002/mp.12810. Epub 2018 Mar 23.
49. Stasi M, Bresciani S, Miranti A, Maggio A, Sapino V, Gabriele P. Pretreatment patient-specific IMRT quality assurance: a correlation study between gamma index and patient clinical dose volume histogram. Med Phys 2012; 39 (12): 7626–7634. doi: 10.1118/1.4767763
50. Kim JI, Park SY, Kim HJ, Kim JH, Ye SJ, Park JM. The sensitivity of gamma-index method to the positioning errors of high-definition MLC in patient-specific VMAT QA for SBRT. Radiat Oncol 2014; 9: 167. doi: 10.1186/1748-717X-9-167
51. Heilemann G, Poppe B, Laub W. On the sensitivity of common gamma-index evaluation methods to MLC misalignments in Rapidarc quality assurance. Med Phys 2013; 40 (3): 031702. doi: 10.1118/1.4789580
52. Fredh A, Scherman JB, Fog LS, Munck af Rosenschöld P. Patient QA systems for rotational radiation therapy: a comparative experimental study with intentional errors. Med Phys 2013; 40 (3): 031716. doi: 10.1118/1.4788645
53. Steers JM, Fraass BA. IMRT QA: selecting gamma criteria based on error detection sensitivity. Med Phys 2016; 43 (4): 1982. doi: 10.1118/1.4943953
54. Lechner W, Primeßnig A, Nenoff L, Wesolowska P, Izewska J, Georg D. The influence of errors in small field dosimetry on the dosimetric accuracy of

https://doi.org/10.1017/S146039692100042X Published online by Cambridge University Press

treatment plans. Acta Oncol 2020; 59 (5): 511–517. doi: 10.1080/0284186X.2019.1685127. Epub 2019 Nov 7.
55. Childress NL, White RA, Bloch C, Salehpour M, Dong L, Rosen II. Retrospective analysis of 2D patient-specific IMRT verifications. Med Phys 2005; 32 (4): 838–850. doi: 10.1118/1.1879272
56. Budgell GJ, Perrin BA, Mott JH, Fairfoul J, Mackay RI. Quantitative analysis of patient-specific dosimetric IMRT verification. Phys Med Biol 2005; 50 (1): 103–119. doi: 10.1088/0031-9155/50/1/009
57. Atiq M, Atiq A, Iqbal K, Shamsi QA, Andleeb F, Buzdar SA. Interpretation of Gamma Index for Quality Assurance of Simultaneously Integrated Boost (SIB) IMRT Plans for Head and Neck Carcinoma. Pol J Med Phys Eng 2017; 23 (4): 93–97.
58. van Zijtveld M, Dirkx ML, de Boer HC, Heijmen BJ. Dosimetric pre-treatment verification of IMRT using an EPID; clinical experience. Radiother Oncol 2006; 81 (2): 168–175. doi: 10.1016/j.radonc.2006.09.008. Epub 2006 Oct 19.

https://doi.org/10.1017/S146039692100042X Published online by Cambridge University Press